

Controlled Growth of Pt-Containing SiO₂ Nanotubes with High Aspect Ratios

Lirong Ren and Michael Wark*

*Institute for Physical Chemistry and Electrochemistry, University of Hanover, Callinstrasse 3-3A,
D-30167 Hanover, Germany*

Received December 27, 2004. Revised Manuscript Received August 10, 2005

Rectangular prisms of [Pt(NH₃)₄](HCO₃)₂ were grown from its aqueous solution by solvent modification with ethanol. The polydispersity of the prisms, being influenced by temperature, the rate of ethanol addition, and the Pt concentration in the aqueous solution, actually results from the iso-oriented aggregation of primary nanofibers into bundles. The employment of prehydrolyzed tetraethyl orthosilicate (TEOS) as a capping agent can effectively stabilize the primary nanofibers. With this stabilized nanofiber as a structure-directing agent, about 100–200 nm thick and up to 40 μ m long SiO₂ nanotubes, which contain up to 40 wt % of Pt, could be synthesized by further addition of TEOS. The capping mechanism of hydrolyzed TEOS can be reasonably explained through the selective adsorption of silanol species on specific surfaces of primary nanofibers. In our method, the ingenious employment of TEOS as the reactant for the nanotube formation and also as a capping agent avoids the introduction of additional substances to the reaction system.

Introduction

Inspired by the wide and highly promising application potentials of carbon nanotubes (CNTs),¹ tubular variants of other materials, also of great interest for fundamentally oriented scientists, have been created in a variety of chemical compositions and in different approaches. Non-carbon NTs exist from metals, like Au² and Te,³ nitrides,⁴ sulfides,⁵ and a number of metal oxides, like V₂O₅, SiO₂, TiO₂, ZrO₂, and MgO. An overview on oxide nanotubes was recently published by Patzke et al.⁶

SiO₂ nanotubes (NTs) have attracted much attention due to the widespread applications of SiO₂ materials in many fields. For example, it is well-known that SiO₂ materials are extensively employed to support metal catalysts (e.g., Pt/SiO₂ catalysts for hydrogenation of hydrocarbons). The increased surface area of SiO₂ materials with a tubular structure in the nanometer regime might lead to unpredictable improvement regarding the catalytic effects. Meanwhile, biochemically modified SiO₂ nanoparticles have shown excellent enzymatic activities and detection capacities due to their large surface areas for enzyme immobilization.⁷ In addition, strong photoluminescence was observed in SiO₂ NTs; hence, applications as light emitters in optical nanodevices were suggested.⁸

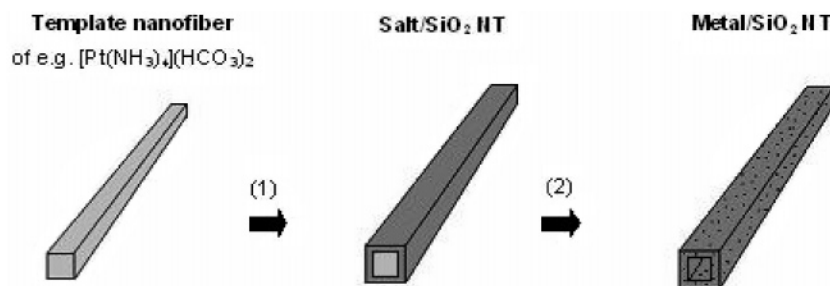
Generally, SiO₂ NTs have been prepared via a template method combined with the sol–gel technique. Because of the ability of sols to condensate on preformed morphologies, the generated SiO₂ NTs represent replicas of the template structures. For example, SiO₂ NTs with tube diameters below 10 nm were produced with templates such as cylindrical micelles of alkylammonium salts⁹ or self-assembled fibril peptides.¹⁰ In the dimension of 30–40 nm, uniform silver nanowires serving as templates were homogeneously coated with SiO₂ shells.¹¹ Further, it was proven that a fibrous metal oxide, V₃O₇·H₂O, could also act as the template to obtain SiO₂ NTs of 50–300 nm in diameter.¹² Moreover, the inner walls of a nanoporous anodic aluminum oxide membrane were explored to act as the template to generate pure SiO₂ NTs with adjustable dimensions.¹³ For these previously mentioned methods, the templates were necessarily removed to generate hollow and pure SiO₂ structures, either by chemical dissolution for the inorganic templates^{11–13} or by a simple calcination for the organic ones.^{9, 10}

Another fascinating aspect of NTs results from the interior cavities, which could be used to incorporate metals for applications (e.g., in catalysis, as nanosensors, and in separation). The procedures to fill NTs might be classified into three groups: (a) filling of pre-synthesized NTs by a wet-chemical method, which leads selectively to a decoration

* To whom correspondence should be addressed. Tel.: 49-511-762-5298. Fax: 49-511-76219121. E-mail: Michael.Wark@pci.uni-hannover.de.

- (1) Ajayan, P. M. *Chem. Rev.* **1999**, 99, 1787.
- (2) Sun, Y.; Mayers, B. T.; Xia, Y. *Nano Lett.* **2002**, 2, 481.
- (3) Mayers, B. T.; Xia, Y. *Adv. Mater.* **2002**, 14, 279.
- (4) Hu, J. Q.; Bando, Y.; Golberg, D.; Liu, Q. L. *Angew. Chem., Int. Ed.* **2003**, 42, 3493.
- (5) Feldman, Y.; Wasserman, E.; Tenne, D.; Srolovitz, R. *Science* **1995**, 267, 222.
- (6) Patzke, G. R.; Krumeich, F.; Nesper, R. *Angew. Chem., Int. Ed.* **2002**, 41, 2446.
- (7) Quobosheae, M.; Santra, S.; Zhang, P.; Tan, W. *Analyst* **2001**, 126, 1274.

- (8) Zhang, M.; Ciocan, E.; Bando, Y.; Wada, K.; Cheng, L. L.; Pirouz, P. *Appl. Phys. Lett.* **2002**, 80, 491.
- (9) Harada, M.; Adachi, M. *Adv. Mater.* **2000**, 12, 839.
- (10) Meegan, J. E.; Aggeli, A.; Boden, N.; Brydson, R.; Brown, A. P.; Carrick, L.; Brough, A. R.; Hussain, A.; Ansell, R. J. *Adv. Funct. Mater.* **2004**, 14, 31.
- (11) (a) Sun, Y.; Gates, B.; Mayers, B.; Xia, Y. *Nano Lett.* **2002**, 12, 165.
(b) Yin, Y.; Lu, Y.; Sun, Y.; Xia, Y. *Nano Lett.* **2002**, 2, 427.
- (12) Zygmunt, J.; Krumeich, F.; Nesper, R. *Adv. Mater.* **2003**, 15, 1538.
- (13) (a) Martin, C. R. *Science* **1994**, 266, 1961. (b) Zhang, M.; Bando, Y.; Wada, K. *J. Mater. Res.* **2000**, 15, 387.

Scheme 1. Illustration of the Synthesis Process of Metal-Containing SiO₂ NTs by the Metal–Salt–Nanofiber Template Method^a

^a (1) Coating of TEOS in a sol-gel process and (2) calcination at 500 °C for 5 h.

of the internal surface,¹⁴ (b) the physical method, where capillarity forces induce the filling of a molten material,¹⁵ and (c) evaporation by arc discharge in an inert atmosphere.¹⁶ In addition, it is noteworthy to mention that Ga-filled MgO single crystalline NTs were prepared by a liquid metal-assisted route and were suggested for application as a wide-range nanothermometer.¹⁷

An alternative metal–salt–nanofiber template method was first established in our group to form SiO₂ and TiO₂ NTs.¹⁸ One typical synthetic procedure is illustrated in Scheme 1. At first, template nanofibers of amino–metal compounds (e.g., [Pt(NH₃)₄](HCO₃)₂) are prepared by a solvent modification process. Afterward, those nanofibers are coated with tetraethyl orthosilicate (TEOS) or tetrabutyl orthotitanate (TBOT). The subsequent calcination at 500 °C reduces the metal ions to metal clusters, which enter the porous SiO₂ or TiO₂ walls or stay inside the tubes. In the case of a Pt salt to TEOS or a TBOT ratio of 1:5, which is the optimum to obtain exclusively NTs, the Pt content in the tubes is up to 40 wt %. In general, the obtained NTs exhibit close ends, although in Scheme 1, an open NT was drawn for clarity.

Compared with other studies mentioned previously, this metal–salt–NF template method is advantageous since it realizes the preparation of NTs as well as the filling with metals simultaneously in an elegant and sufficient way. The easily achievable high amount of metal filling can provide many potential applications to the oxide NTs. For the thus-synthesized SiO₂ NTs, gas adsorption and catalytic properties different from that of ordinarily supported Pt–SiO₂ catalysts prepared by the aqueous impregnation method¹⁹ are expected

since a large amount of Pt particles is freely anchored inside the tubes and, thus, is very accessible to reactants as already proven by the adsorption of CO.^{18f} An even more promising observation with respect to anisotropic electric conductivity is the formation of continuous Pt nanowires that mostly are found in the thinnest SiO₂ NTs.^{18e} For thus-synthesized titania NTs,^{18a} doping by Pt metals could improve the conductivity of semiconductor titania, rendering this kind of NTs as a potential application in nanoelectronics. Recently, this template method was also applied to synthesize alumina and silica–alumina NTs filled with Pt particles, and the latter may exhibit characteristic acidic properties.²⁰ Other metals including Pd and Co have also been successfully encapsulated into SiO₂ and SiO₂/TiO₂ NTs with this metal–salt–nanofiber template method in our laboratory.²¹ Hence, it is very promising to develop this facile template method for the routine fabrication of metal-containing oxide nanotubes.

In this template method, the precipitation of single thin metal salt fibers from aqueous solution is the decisive step to achieve optimum morphology of the final NTs. Perfect control of two fundamental steps (nucleation and growth) is important. During precipitation, the simultaneous control of dimension, morphology, and monodispersity is the most important issue for the synthesis of nanostructures.²² To control the size and shape of 1-D nanostructures, Peng and co-workers pioneered the growth of monodisperse CdSe nanorods with a well-controlled aspect ratio by using mixed surfactants (trioctyl phosphine oxide and hexyl-phosphonic acid) as capping reagents.²³ In comparison, suffering on a lack of careful control on the morphology of the metal–salt–NF used as a template, our early syntheses comprised SiO₂ NTs with a broad size distribution in the diameter dimension.

On the basis of our latest efforts, the polydispersity of the template results from the iso-oriented aggregation of primary nanofibers, a phenomenon also found for, for example, copper oxalate,²⁴ iron oxide,²⁵ and cerium oxide.²⁶ The employment of pre-hydrolyzed TEOS as a capping agent has

- (14) (a) Grubert, G.; Rathousky, J.; Schulz-Ekloff, G.; Wark, M.; Zukal, A. *Microporous Mesoporous Mater.* **1998**, *22*, 225. (b) Yang, B.; Kamiya, S.; Shimizu, Y.; Koshizaki, N.; Shimizu, T. *Chem. Mater.* **2004**, *16*, 2826.
- (15) (a) Ugarte, D.; Stöckli, T.; Bonard, J. M.; Châtelain, A.; de Heer, W. A. *Appl. Phys.* **1998**, *A67*, 101. (b) Dujardin, E.; Ebbesen, T. W.; Hiura, H.; Tanigaki, K. *Science* **1994**, *265*, 1850.
- (16) Saito, Y.; Nishikubo, K.; Kawabata, K.; Matsumoto, T. *J. Appl. Phys.* **1996**, *80*, 3062.
- (17) Li, Y. B.; Bando, Y.; Golberg, D.; Liu, Z. W. *Appl. Phys. Lett.* **2003**, *83*, 999.
- (18) (a) Hippe, C.; Wark, M.; Lork, E.; Schulz-Ekloff, G. *Microporous Mesoporous Mater.* **1999**, *31*, 235. (b) Wark, M.; Hippe, C.; Schulz-Ekloff, G. *Stud. Surf. Sci. Catal.* **2000**, *129*, 475. (c) Ren, L.; Melville, U.; Wark, M. *Frontiers of Solid State Chemistry*; World Scientific Publishing, Ltd.: Singapore, 2002; 441. (d) Zygmunt, J.; Krumeich, F.; Muhr, H.-J.; Nesper, R.; Ren, L.; Wark, M. *Z. Anorg. Allg. Chem.* **2002**, *628*, 2189. (e) Krumeich, F.; Wark, M.; Ren, L.; Muhr, H.-J.; Nesper, R. *Z. Anorg. Allg. Chem.* **2004**, *630*, 1054. (f) Hippe, C. Ph.D. Thesis, University of Bremen, 2000; p 58.
- (19) Dias, E.; Davies, A. T.; Mantle, M. D.; Roy, D.; Gladden, L. F. *Chem. Eng. Sci.* **2003**, *58*, 621.

- (20) Miyao, T.; Saika, T.; Saito, Y.; Naito, S. *J. Mater. Sci. Lett.* **2003**, *22*, 543.
- (21) Ren, L.; Wark, M., unpublished results.
- (22) Xia, Y.; Yang, P.; Sun, Y.; Wu, Y.; Mayers, B.; Gates, B.; Yin, Y.; Kim, F.; Yan, H. *Adv. Mater.* **2003**, *15*, 353.
- (23) Peng, X.; Manna, L.; Yang, W.; Wickham, J.; Scher, E.; Kadavanich, A.; Alivisatos, A. P. *Nature* **2000**, *404*, 59.
- (24) Jongen, N.; Bowen, P.; Lemaître, J.; Valmalette, J.; Hofmann, H. J. *Colloid Interface Sci.* **2000**, *226*, 189.
- (25) Matijevic, E.; Sheiner, P. *J. Colloid Interface Sci.* **1978**, *63*, 509.
- (26) Hsu, W. P.; Ronquist, L.; Matijevic, E. *Langmuir* **1988**, *4*, 31.

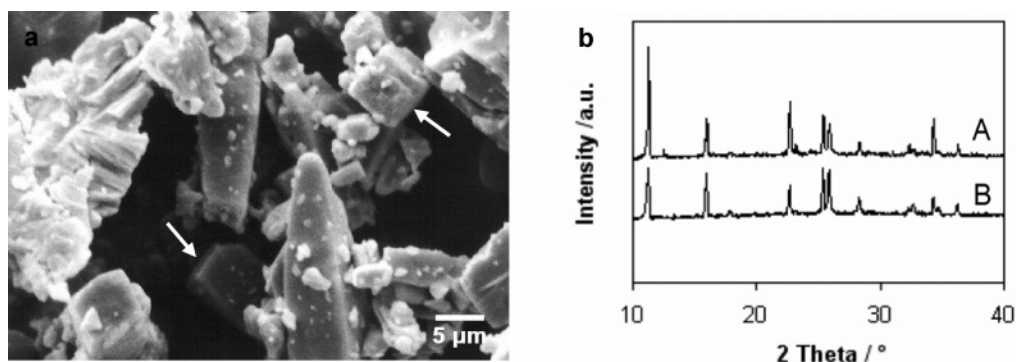


Figure 1. (a) SEM image of commercial $[\text{Pt}(\text{NH}_3)_4](\text{HCO}_3)_2$ and (b) the XRD patterns of both the commercial salt (A) and the Pt salt template (B).

effectively stabilized the primary nanofibers, leading to the controlled growth of Pt-containing (ca. 40 wt %) silica nanotubes with much improved monodispersity (100–200 nm in diameter) and lengths up to 40 μm , resulting in aspect ratios of 100–400. According to our knowledge, no other such simple solution-phase method leads to SiO_2 NTs with such high aspect ratios.

Experimental Procedures

Chemicals. $[\text{Pt}(\text{NH}_3)_4](\text{HCO}_3)_2$ (Chempur), TEOS (>98%, Merck) was used without any further purification. For the preparation of an ammonia solution (pH = 10–11, 20 $^\circ\text{C}$), 1 mL of saturated ammonia solution (p.a., Merck) was diluted to 100 mL with distilled water.

Study on the Polydispersity of $[\text{Pt}(\text{NH}_3)_4](\text{HCO}_3)_2$ Template. Under vigorous stirring, 0.0125 mmol of $[\text{Pt}(\text{NH}_3)_4](\text{HCO}_3)_2$ was dissolved in 1 mL of aqueous ammonia solution to form the mother solution, to which afterward ethanol was dropped. Along with the addition of ethanol, the mother solution turned from a transparent colorless solution to a white cloudy suspension. Different parameters including temperature (0 $^\circ\text{C}$ and room temperature), the rate of ethanol addition (0.5, 10, and 1000 mL/min), Pt salt concentration in the mother solution (0.001, 0.003, and 0.0125 M), and ratio of ethanol to water (1:1 and 10:1) were addressed.

Synthesis of Monodisperse and Ultralong SiO_2 NTs. With a stirring rate of 300 rpm, 0.0125 mmol of $[\text{Pt}(\text{NH}_3)_4](\text{HCO}_3)_2$ was dissolved in 1 mL of ammonia solution, and then 0.7 mL of ethanol was added into the solution. Afterward, the system was kept inside an ice bath (ca. 0 $^\circ\text{C}$) for 8 min, then 14 μL of TEOS was added, and the whole system was stirred for a short time. With an increased stirring rate of 1000 rpm, a small amount of ethanol was injected rapidly into the mixture, and several minutes later, the stirring rate was decreased to 300 rpm, and 10 mL of ethanol was added slowly into the reaction system. When the addition of ethanol was finished, more TEOS could be added according to requirements (i.e., the envisaged Si/Pt ratio). Monodisperse and ultralong SiO_2 NTs were achieved after 4 h of stirring. The sample was dried naturally in air and calcined at 500 $^\circ\text{C}$ for 5 h (heating rate: 5 $^\circ\text{C}/\text{min}$, air).

Characterization. Scanning electron microscopy (SEM) was performed on a JSM-6700F microscope (JEOL, $V_{\text{acc}} = 2$ kV). To retain the original morphology of the sample, the suspension was directly dropped on a sample holder and analyzed after evaporation of the solvents. For transmission electron microscopy (TEM), the calcined sample was deposited on a carbon foil supported by a copper grid. The TEM image was recorded on a CM30 microscope (Philips, $V_{\text{acc}} = 300$ kV, LaB_6 cathode) or on a JEOL-2100F ($V_{\text{acc}} = 200$ kV, FET cathode). The powder X-ray diffraction (XRD) patterns of samples were recorded on a Philips PW 1729 spec-

trometer (Bragg–Brentano parafocusing geometry, $\lambda = 1.5418$ \AA , voltage = 35 kV, and current intensity = 40 mA).

Results and Discussion

Study on the Polydispersity of the Pt Salt Template. A SEM image of commercially available $[\text{Pt}(\text{NH}_3)_4](\text{HCO}_3)_2$ is shown in Figure 1a for comparison. The particles are larger than 5 μm . Some particles show rectangular edges (indicated by arrows), although most of them are not regular. Figure 1b shows the XRD patterns of the commercial salt and the Pt salt template fibers prepared by dissolution of the commercial salt in water and reprecipitation (solvent modification from water to ethanol) of the Pt salt, $[\text{Pt}(\text{NH}_3)_4](\text{HCO}_3)_2$. The identical two powder XRD patterns indicate that the chemical composition of the Pt salt template agrees very well with that of the commercial $[\text{Pt}(\text{NH}_3)_4](\text{HCO}_3)_2$.

To achieve suitable templating structures for the formation of uniform nanotubes, the Pt salt nanofibers have to be formed as homogeneously as possible. It was found that the morphology of the precipitated $[\text{Pt}(\text{NH}_3)_4](\text{HCO}_3)_2$ nanofibers depends on a number of parameters (i.e., temperature, Pt salt concentration in the aqueous mother solution, ratio of ethanol to water, and the rate of ethanol addition). In general, the applied process of solvent modification is very simple since there is a strong tendency of the tetraamminoplatinum salt to grow with a 1-D morphology. This habit is attributed to the highly anisotropic bonding in the crystallographic structure^{18a} similar to the situation in asbestos and chrysotile.²⁷

The temperature of reprecipitation has a strong influence on the polydispersity of the Pt salt template; the lower the temperature, the lower the thickness of the precipitated fibers, whereas at 20 $^\circ\text{C}$, fibers with a thickness of up to 3–5 μm were found at 0 $^\circ\text{C}$, and their diameter was limited to about 1–2 μm . The lower thickness and the combined narrower size distribution of the fibers prepared at 0 $^\circ\text{C}$ might, in principle, be a result of smaller-sized nuclei at lower temperatures. However, less aggregation of primary nanofibers seems to be more important as shown next. The relative decrease in length of the fibers at 0 $^\circ\text{C}$ can be ascribed to an increase in the number of nuclei leading to the growth of smaller fibers. Unfortunately, it is not feasible to obtain monodisperse nanofibers by further cooling the system

(27) Noll, W. Z. *Anorg. Chem.* **1950**, 261, 1.

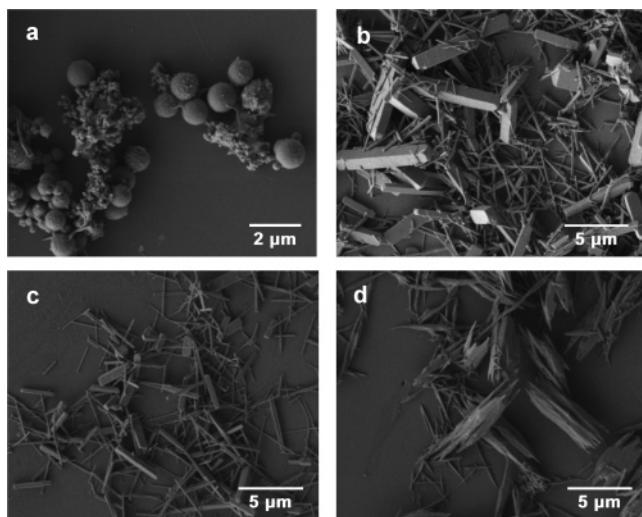


Figure 2. Representative SEM micrographs of Pt salt templates prepared at 0 °C and at an ethanol addition rate of 10 mL/min with different salt concentrations in the aqueous solution and different water/ethanol ratios: (a) Pt salt concentration 0.001 M, water/ethanol ratio 1:10; (b) 0.003 M, 1:10; (c) 0.0125 M, 1:10; and (d) 0.0125 M, 1:1.

because the aqueous solution system begins to freeze out not far below 0 °C.

The Pt salt concentration in the aqueous mother solution is also of great influence on the polydispersity of the Pt salt template. As long as the Pt salt concentration is as low as 0.001 M, no 1-D fibers are formed, and as a consequence, instead of nanotubes only SiO₂ nanospheres (0.3–1.0 μm in diameter) are found after the addition of TEOS to such a template solution (Figure 2a). The observed formation of the nanospheres follows the rules developed by Stöber et al.²⁸ 1-D fibers of the template salt were obtained if the salt concentration in the aqueous solution was at least 0.003 M. However, in the concentration range of 0.003–0.005 M, the few thin Pt salt nanofibers were accompanied by a large number of very large particles or microfibers (Figure 2b). If the Pt salt concentration in the aqueous solution was increased from 0.005 to 0.0125 M, the relative amount of nanofibers in the template mixture increased, and the microfibers formed decreased in number and size (Figure 2c). It is obvious that the concentration of the Pt salt must be high enough to create a high number of nucleation seeds already forming when the first drops of ethanol are added. One has to keep in mind that the precipitation is induced just by the dilution of water acting as a good solvent for the platinum salt by the worse solvent ethanol. To achieve fast growth of the first precipitated nuclei and to avoid formation of new nuclei, the rate of ethanol addition must be high. If other factors are kept constant and the rate of ethanol addition is increased from 0.5 to 10 mL/min, the number of micrometer thick fibers appearing in the template mixture decreases continuously. Rates higher than 10 mL/min do not lead to further improvement, and for concentrations of the Pt salt in the mother solution higher than 0.0125 M, the size distribution even became worse, probably because the concentration of Pt ions is locally so high that not enough Pt salt precipitates during the first addition of ethanol, and

consequently, new nucleation seeds are formed during the prolonged ethanol addition. But even by use of the optimum concentration of 0.0125 M Pt-salt in the mother solution and a high rate of ethanol addition, a broad size distribution of the templating salt cannot be fully avoided (Figure 2c). Also, at these conditions, some fibers with a thickness of up to 1 μm are found in the SEM pictures.

The mechanism of the formation of these thick fibers can be deduced by varying the ethanol/water ratio in the Pt salt suspension. Typically, this ratio is 1:10 to achieve complete precipitation of all the Pt salt. If the ethanol addition is early interrupted at a ethanol/water ratio of 1:1, it can be seen on the SEM micrograph shown in Figure 2d that again nanofibers are not the only morphology but that they are accompanied by bundles of nanofibers. In these bundles, the primary nanofibers are still observable. The lateral aggregation of as-grown nanofibers to bundles with a width of about 1 μm takes place to minimize the surface energy. The big bundles show already smooth sides but rather rugged ends. Because of further precipitation of Pt salt from solution, these rugged ends are smoothed during the addition of more ethanol. In crystallization processes, steps and kinks are always the preferred places for ions from solution to attach.

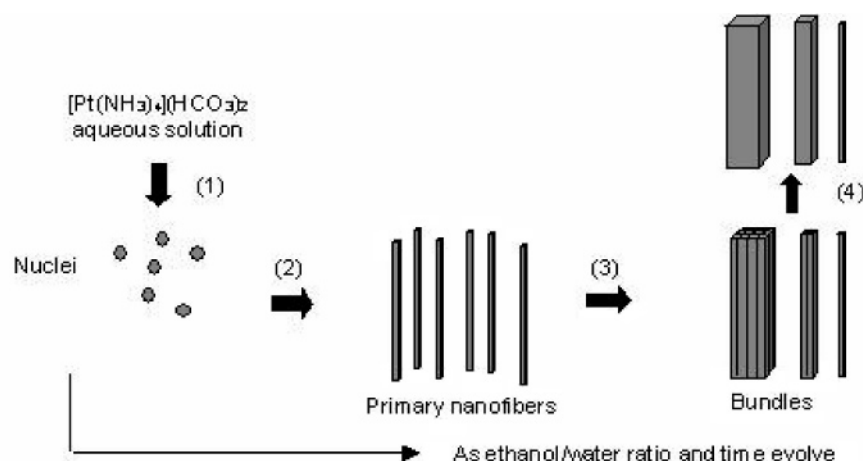
Formation Mechanism of the Polydisperse Pt Salt Template. The formation of the Pt salt template (Scheme 2) follows a similar procedure as the aggregation-mediated crystal growth nucleation,^{24,29,30} anisotropic growth, iso-oriented aggregation, and aging. Along with the dropwise addition of ethanol for the Pt salt, a state of supersaturation is reached due to its poor solubility in ethanol. Once the concentration of building blocks (ions) becomes sufficiently high, they aggregate into small clusters (nuclei) through a homogeneous nucleation. Since the surface energies of the nuclei are different, with continuously providing building blocks, the nuclei serve as seeds for further anisotropic growth, and monodisperse primary nanofibers (50–100 nm in width) are formed. Since the unit cell of the [Pt(NH₃)₄](HCO₃)₂ salt is slightly enlarged in the *c*-direction,^{18a} the (001) face might possess the highest surface energy and, consequently, grows faster. If the preferred growth into one direction has started, the attachment of further nuclei leading to imperfections on the growing face even enhances the growth. Therefore, long and thin fibers are formed.

However, these primary nanofibers grown at the initial stage do not keep their independency from each other but feature a strong tendency to aggregate into iso-oriented bundles. It can be assumed that the rate of nucleation and growth of the primary nanofibers is constant throughout the aggregation process, so that the continuous supply of primary particles compensates for their consumption and polydispersity (0.05–2 μm, approximately) in aggregate size increases. Defects or initial mismatches at the particle–particle interfaces disappear during the aging process. The iso-oriented aggregation of primary nanofibers is controlled by a type of electrostatically assisted van der Waals interaction in aqueous medium. Aggregation of fibers to larger

(28) Stöber, W.; Fink, A.; Bohn, E. *J. Colloid Interface Sci.* **1968**, *26*, 62.

(29) Mann, S.; Cölfen, H. *Angew. Chem., Int. Ed.* **2003**, *42*, 2350.

(30) LaMer, V. K.; Dinegar, R. H. *J. Colloid Interface Sci.* **1980**, *76*, 418.

Scheme 2. Illustration of the Formation Mechanism of Polydisperse Pt Salt Template^a

^a Iso-oriented aggregation of primary nanofibers leads to a polydisperse system. (1) nucleation, (2) anisotropic growth, (3) iso-oriented aggregation, and (4) aging.

particles to minimize surface energy is a well-known phenomenon.²⁴ Zeta potential measurements indicated that in the sum, the lateral faces of primary nanofibers are almost neutral. This, however, does not rule out that some faces are terminated by $[\text{Pt}(\text{NH}_3)_4]^{2+}$ cations and others by HCO_3^- ions. An electrostatic attraction results, and thus, the nanofibers are attracted to one another and laterally fuse together along a common crystallographic axis. Since the fiber diffusion and the mobility of primary attached H_2O or ethanol molecules is higher at increased temperatures, helping to strip the dipole molecules off, aggregation between nanofibers is more pronounced at 20 °C than at 0 °C. With the propagation of time, going in line with the addition of more ethanol, more primary Pt salt particles from solution are attached to the kinks at the first formed bundles of nanofibers, and consequently, the edges of the bundles are smoothed.

Controlled Growth of Monodisperse SiO_2 NTs. It is proven in this work that aggregation of primary nanofibers can be suppressed sufficiently by the capping effect of hydrolyzed TEOS, leading to a controlled growth of monodisperse SiO_2 NTs. The strategy for the controlled synthesis was developed as follows: TEOS was added into the mother solution before the formation of the template and allowed to undergo a short period of intensive hydrolysis. Afterward, at an extremely rapid stirring rate (e.g., 1000 rpm), a pulse of ethanol was injected into the already saturated solution. A short period for a focusing process²³ of nuclei is needed for homogeneous nucleation. Then, the stirring rate was decreased to the typical one (e.g., 300 rpm), and a large amount of ethanol was pumped with a rather slow rate into the nuclei-abundant suspension, for the purpose of providing a well-controlled slow supply of building blocks for the anisotropic growth of template nanofibers. Because of the presence of hydrolyzed TEOS in the suspension anchoring at the surface of the nanofibers, the aggregation of nanofibers has been prohibited.

Figure 3 shows the template-filled sample prepared by the controlled growth, featuring high aspect ratios (up to 40 μm in length, Figure 3a) and a narrow size distribution (100–200 nm in the outer diameters, Figure 3b). After the calcination at 500 °C for 5 h in air, the structure-directing

Pt salt template was reduced, and at the end, Pt-containing SiO_2 NTs resulted. As shown by a typical dark-field TEM image in Figure 3c, monodisperse crystalline Pt nanoparticles (1–3 nm) are evenly distributed in the wall. Because of the rectangular cross-section of the tube, the Pt density is higher at the edges than in the center area since at the edges the electrons pass more wall material. Inside the thinnest NTs, continuous Pt nanowires are observed (Figure 3d). The relative short length (2–3 μm) of the relatively thin NTs probably results from a mechanical abrasion during the sample preparation for the TEM measurement.

The observation of a bundle of SiO_2 NTs, as depicted in Figure 4, confirms the authenticity of the iso-oriented aggregation of primary nanofibers (illustrated in Scheme 2). The relative amount of bundles of NTs in one sample could be greatly varied by changing the prehydrolysis time of TEOS. The optimized prehydrolysis time was 2 min at 0 °C without significant observations of bundles. When the prehydrolysis time was set to 1 min, the amount of bundles was about 50%. The shorter the prehydrolysis time, the higher the relative amount of bundles is. Further specific studies on this aspect will be carried out since the bundles of SiO_2 NTs, as the result of a self-assembly process, might offer interesting applications (e.g., the development of membranes).

In the present system, hydrolyzed TEOS was used as a capping agent and succeeded not only in limiting the aggregation among monodisperse primary nanofibers but also in promoting the anisotropic growth of Pt-containing SiO_2 NTs. The supposed function of capping agents was the kinetic control of the growth rate of various faces by interacting with these faces through adsorption and desorption, as is the case of silver nanowires by poly(vinyl pyrrolidone) (PVP)¹¹ and CdSe²³ or Co nanorods³¹ by trioctyl phosphine oxide. Upon the pre-addition, TEOS undergoes a rapid hydrolysis in the environment of ammonia solution, water, and ethanol, producing a large amount of silanol monomers in a form of $(\text{RO})_x\text{Si}(\text{OH})_x$ (x varies from 1 to

(31) Puentes, V. F.; Krishnan, K. M.; Alivisatos, A. P. *Science* **2001**, 291, 2115.

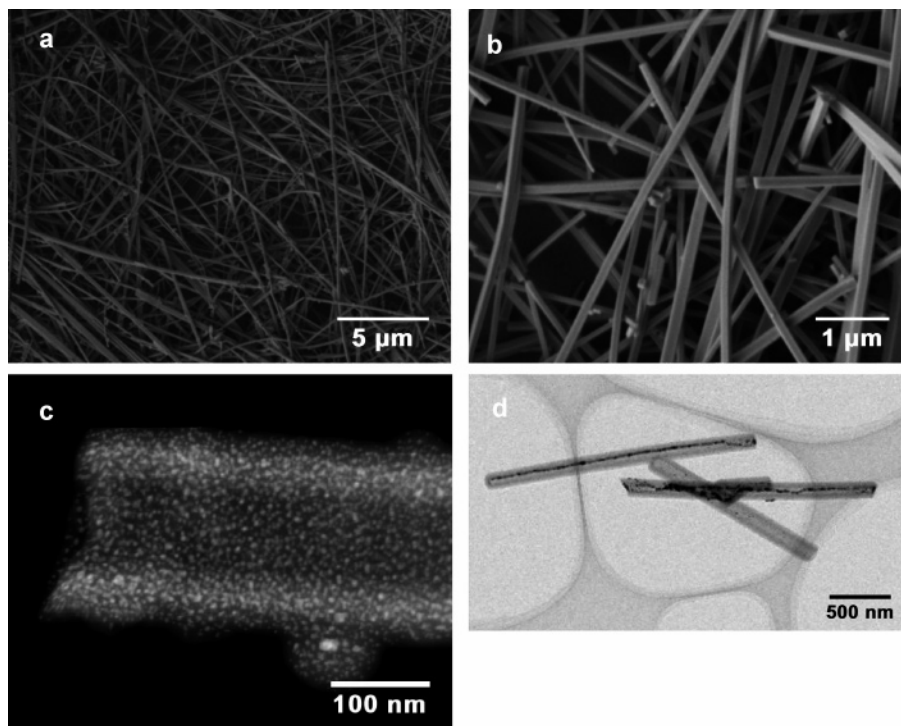


Figure 3. SEM images of SiO₂ NTs showing (a) the high aspect ratios and (b) monodispersity. Typical TEM images (c and d) of Pt-containing SiO₂ NTs after calcination.

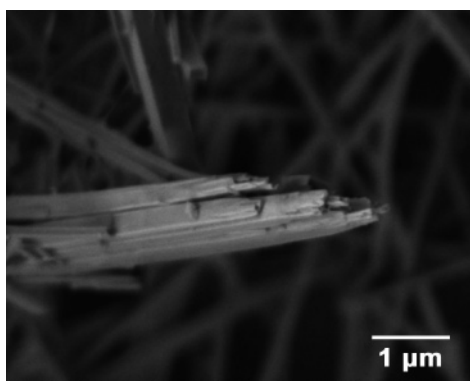


Figure 4. SEM image of a bundle of SiO₂ NTs.

4). The silanol monomers would be deprotonated at the basic condition and are therefore mutually repulsive and are relatively stable according to the DLVO (Derjaguin, Landau, Verwey, and Overbeek) theory.³² However, the duration of the hydrolysis must be controlled on one hand because at pH = 10–11 (0 °C), the condensation between silanol monomers is still relatively fast and should be avoided and on the other hand since the double layer repulsion is greatly reduced with the presence of electrolyte (i.e., [Pt(NH₃)₄](HCO₃)₂). When nuclei appear upon the injection of ethanol, the deprotonated monomer or oligomer silica ions are adsorbed to a larger extent than water and ethanol molecules on the specific facets of nuclei or the nanofibers. This is in accordance with Lundelius's rule,³⁴ which claims that the extent of adsorption is usually higher from solvents in which the adsorptive is less soluble. The interaction between the

silica species and the nanofibers results from the electrostatic forces between the slightly cation-terminated faces of the [Pt(NH₃)₄](HCO₃)₂ fibers and the negatively charged SiO₄H_x^{(4-x)-} monomers or Si_xO_yH_zⁿ⁻ oligomers assisted by hydrogen bonding with the amine groups of the salt as hydrogen donor and the oxygen in the silica ions as hydrogen acceptor and, probably also important, by an ion exchange of the hydrogen carbonate ions and the silicate ions. Small amounts of hydrogen carbonate ions could be detected in the solutions.

With a suitable supply of building blocks by ethanol addition, the fibers attach further nuclei in growth direction without adsorption of silica species on the growing face. An adsorptive layer of silica species is, however, simultaneously attached at the lateral faces perpendicular to the face at which the crystal growth proceeds. The attachment of a silica species to the lateral faces is preferred to the adsorption of ethanol and water molecules due to the Coulomb forces between the silica anions and the positively charged surface of the salt. As a consequence, the resulting anion termination of the capped fibers prevents their agglomeration.

In addition, there is lateral growth of the silica layer by further condensation of silanol species. Gradually, with the 1-D growth on one hand, and the lateral layer growth on the other, the final template-containing SiO₂ NTs are formed. The formation of the bundle of SiO₂ NTs, observed for short prehydrolysis periods (Figure 4), occurs due to the insufficient capping of Pt salt nanofibers during fast anisotropic growth. This indicates that the hydrolysis and early condensation of TEOS leading to the formation of negatively charged ions needs some time.

To a certain extent, the capping effect of TEOS is comparable with its coating effect that has been very widely employed to coat any preformed morphologies, but what has

(32) Brinker, C. J.; Scherer, G. W. *Sol–Gel Science: the Physics and Chemistry of Sol–Gel Processing*; Academic Press: Boston, 1990.

(33) Ross, S.; Morrison, I. D. *Colloidal Systems and Interfaces*; Wiley: New York, 1988.

been demonstrated here is its selective coating in this particular system of 1-D growth of the nanostructures. In the modified growth route, the two functions of TEOS were elegantly combined together to yield the shapely product. Compared with using conventional surfactants,^{12,31,32} the ingenious employment of the reactant itself (TEOS) as a capping agent in our method avoided the introduction of additional substances to the reaction system.

Conclusions

Formation of the Pt salt template for preparation of Pt-containing SiO₂ NTs has been systematically investigated by varying parameters such as temperature, the rate of ethanol addition, Pt salt concentration, and the ratio of ethanol to water. The thickness distribution of the rectangular fibers of Pt salt prepared by a solvent modification decreases with the decrease of temperature and the increase of the rate of ethanol addition and Pt salt concentration in the mother solution. The polydispersity of the Pt salt template results

from an iso-oriented aggregation of primary nanofibers, which is an electrostatically induced self-assembly process driven by the higher surface energy of the lateral faces.

Furthermore, monodisperse and ultralong Pt-containing SiO₂ NTs have been prepared in a kinetically controlled route. During the advanced preparation, TEOS was employed not only as a coating agent to form the tube walls but also as a capping agent to prevent the primary nanofibers of the Pt salt from iso-oriented aggregation. The capping mechanism of hydrolyzed TEOS was reasonably explained through the selective adsorption of silica ions on lateral surfaces of the primary nanofibers.

Acknowledgment. The authors thank Dr. Frank Krumeich (ETH Zurich, Switzerland) for recording the TEM micrographs, Dr. Xiaobo Yang for the XRD measurement, and Dr. Armin Feldhoff for inspiring discussions. Support from the Deutsche Forschungsgemeinschaft (DFG, WA 1116-5 and WA 1116-8) is gratefully acknowledged.

CM047733T